*Entropy* **2014**, *16*, 4839-4854; doi:10.3390/e16094839

OPEN ACCESS

*entropy*

**ISSN 1099-4300**

www.mdpi.com/journal/entropy

*Article*

# Low-Pass Filtering Approach via Empirical Mode Decomposition Improves Short-Scale Entropy-Based Complexity Estimation of QT Interval Variability in Long QT Syndrome Type 1 Patients

**Vlasta Bari [1], Andrea Marchi [2], Beatrice De Maria [3], Giulia Girardengo [4,5], Alfred L. George Jr [6,7], Paul A. Brink [8], Sergio Cerutti [9], Lia Crotti [4,5,10], Peter J. Schwartz [4] and Alberto Porta [11,12,*]**

1 Department of Cardiothoracic, Vascular Anesthesia and Intensive Care, IRCCS Policlinico San Donato, Via Morandi 30, 20097 San Donato Milanese, Milan, Italy; E-Mail: vlasta.bari@grupposandonato.it

2 Department of Anesthesia and Intensive Care Unit, Humanitas Clinical and Research Center, Via Manzoni 56, 20089 Rozzano, Italy; E-Mail: marchi.andrea1@gmail.com

3 IRCCS Maugeri Foundation, 20138 Milan, Italy; E-Mail: beatrice.demaria@mail.polimi.it

4 Center for Cardiac Arrhythmias of Genetic Origin, IRCCS Istituto Auxologico Italiano, Centro Diagnostico San Carlo, Via Pier Lombardo 22, 20135 Milan, Italy; E-Mails: giuliagira82@yahoo.it (G.G.); liacrotti@yahoo.it (L.C.); peter.schwartz@unipv.it (P.J.S.)

5 Department of Molecular Medicine, University of Pavia, 27100 Pavia, Italy

6 Department of Pharmacology, Northwestern University Feinberg School of Medicine, Chicago, IL 60611, USA; E-Mail: al.george@northwestern.edu

7 Department of Medicine and Pharmacology, Vanderbilt University, Nashville 37232, TN, USA

8 Department of Internal Medicine, University of Stellenbosch, Matieland, 7602, Stellenbosch, South Africa; E-Mail: pab@sun.ac.za

9 Department of Electronics, Information, and Bioengineering, Politecnico di Milano, Piazza Leonardo da Vinci 32, 20133 Milan, Italy; E-Mail: sergio.cerutti@polimi.it

10 Institute of Human Genetics, Helmholtz Zentrum München, Ingolstädter Landstraße 1, 85764 Neuherberg, Germany

11 Department of Biomedical Sciences for Health, University of Milan, Via R. Galeazzi 4, 20161 Milan, Italy

12 IRCCS Galeazzi Orthopedic Institute, Via R. Galeazzi 4, 20161 Milan, Italy

* Author to whom correspondence should be addressed; E-Mail: alberto.porta@unimi.it; Tel.: +39-02-50319976; Fax: +39-02-50319960.

*Received: 11 July 2014; in revised form: 20 August 2014 / Accepted: 01 September 2014 / Published: 5 September 2014*

**Abstract:** Entropy-based complexity of cardiovascular variability at short time scales is largely dependent on the noise and/or action of neural circuits operating at high frequencies. This study proposes a technique for canceling fast variations from cardiovascular variability, thus limiting the effect of these overwhelming influences on entropy-based complexity. The low-pass filtering approach is based on the computation of the fastest intrinsic mode function via empirical mode decomposition (EMD) and its subtraction from the original variability. Sample entropy was exploited to estimate complexity. The procedure was applied to heart period (HP) and QT (interval from Q-wave onset to T-wave end) variability derived from 24-hour Holter recordings in 14 non-mutation carriers (NMCs) and 34 mutation carriers (MCs) subdivided into 11 asymptomatic MCs (AMCs) and 23 symptomatic MCs (SMCs). All individuals belonged to the same family developing long QT syndrome type 1 (LQT1) via *KCNQ1*-A341V mutation. We found that complexity indexes computed over EMD-filtered QT variability differentiated AMCs from NMCs and detected the effect of beta-blocker therapy, while complexity indexes calculated over EMD-filtered HP variability separated AMCs from SMCs. The EMD-based filtering method enhanced features of the cardiovascular control that otherwise would have remained hidden by the dominant presence of noise and/or fast physiological variations, thus improving classification in LQT1.

**Keywords:** heart rate variability; LQT1; EMD; sample entropy; *KCNQ1*-A341V mutation; beta-blocker therapy; autonomic nervous system; cardiovascular control

## 1. Introduction

Long QT syndrome type 1 (LQT1) is an inherited disease affecting the delayed slow rectifier potassium current $I_{Ks}$ of the cardiac cells. The most visible effect of this pathology on the surface electrocardiogram is the prolongation of the QT interval accompanied by its maladjustments to heart period (HP) changes [1,2]. As a consequence, in the presence of a tachycardic run, LQT1 patients have a greater likelihood that the incoming cardiac depolarization occurs when the ventricular repolarization process is not concluded, and this phenomenon promotes the development of lethal arrhythmias.

While genetic mutations underpinning LQT1 have been recognized [2] and the administration of beta-blockers, lengthening HP and reducing HP variability, is an effective therapy [3], the attention of the scientific community has recently moved towards factors modifying the arrhythmic risk of LQT1 patients [4–7]. Indeed, within a group of mutation carriers (MCs) presenting the same genotype, two different phenotypes might be detected, leading to completely different clinical outcomes: asymptomatic MCs (AMCs), who did not develop any major cardiac arrhythmias and, thereby, are at low cardiac risk, and symptomatic MCs (SMCs), who experienced episodes of cardiac arrest and syncope and, thereby, are at high cardiac risk. Recent studies pointed out the role of the autonomic nervous system in modulating the cardiac risk of LQT1 patients [8,9]. Indeed, it was found that AMCs feature a low baroreflex sensitivity [8] and a smaller HP prolongation after an exercise stress test [9] compared to SMCs, thus suggesting that a less reactive vagal control directed to the sinus node is a

protective factor. Even more recently, we found that AMCs exhibit a lower complexity of the QT variability at long time scales [10], as assessed from multiscale entropy analysis [11,12], compared to SMCs, thus suggesting that a less complex sympathetic control directed to ventricles is a protective factor and stressing the clinical relevance of the assessment of complexity indexes from QT variability in LQT1 [10].

Unfortunately, automatic QT measurement is a complicated task due to the difficulty in defining the T-wave end, especially in 24-hour Holter recordings with low temporal resolution and in pathological individuals exhibiting abnormal ventricular repolarization [13]. As a consequence, QT variability is affected by broad band noise and has a low signal-to-noise ratio, which might prevent any differentiation between AMCs and SMCs. As a matter of fact, multiscale entropy analysis [11,12] allowed the separation between AMCs and SMCs at long time scales due to its intrinsic ability to filter fast QT variations when long time scales are under scrutiny [10].

The aim of this study is to provide a method to filter out fast fluctuations of QT variability and to allow the separation among groups having different cardiac risk using complexity analysis, even at short time scales, thus rendering unnecessary the application of the multiscale entropy and simplifying the process of LQT1 risk stratification based on complexity analysis. This method is based on the empirical mode decomposition (EMD) [14], allowing the decomposition of the QT variability into oscillatory modes, called intrinsic mode functions (IMFs), and on the evaluation of complexity at short time scales based on sample entropy (SampEn) [15]. EMD has been extensively applied to cardiovascular variabilities, especially to HP dynamics [16–18], with relevant findings in risk stratification of chronic heart failure patients [19]. SampEn is a widely-accepted method for the assessment of the complexity of the cardiac control, and it has been extensively validated compared to other entropy-based metrics [20,21]. We hypothesize that the fastest IMF computed over QT variability provides a good description of the superimposed noise. Therefore, we propose to perform traditional complexity analysis at short time scales using SampEn over the original QT variability after having canceled the fastest IMF. We applied this procedure to QT variability derived from 24-hour Holter recordings obtained from non-MCs (NMCs) and MCs, all belonging to a South African founder population with LQT1 due to the *KCNQ1*-A341V mutation [22,23]. The procedure was applied to the HP variability series, as well. We assessed the ability of the method to distinguish NMCs from MCs, divided into AMCs and SMCs, and to study the effect of beta-blocker therapy (BB) in AMCs and SMCs. The contribution of the autonomic nervous system to the original QT and HP series and their EMD-filtered versions were evaluated, as well, by comparing recordings obtained daytime (DAY) and nighttime (NIGHT) in both AMCs and SMCs.

## 2. Methods

### *2.1. EMD-Based Filtering Approach*

Given the time series $x = \{x(i), i = 1, \ldots, N\}$ with $x$ = HP or QT, where $i$ is a progressive cardiac beat number and $N$ is the series length, EMD is a technique allowing the decomposition of the signal into IMFs from the shortest to the longest time scale [14]. IMFs are characterized by the symmetry with respect to zero, the uniqueness of the local frequency and the impossibility for different modes to

share the same frequency at the same time. The method is based on an iterative procedure composed by several steps: (1) the identification of all the extrema (maxima and minima) of $x$; (2) the generation of the upper and lower envelope of $x$ via cubic spline interpolation among all maxima and minima of $x$, respectively; (3) point-by-point averaging of the two envelopes to compute the local mean series $m$; (4) subtraction of $m$ from $x$ to obtain a mode candidate $h$ (*i.e.*, $h(i) = x(i) - m(i)$); (5) if $h$ did not satisfy the previously defined properties necessary to be an IMF, $x$ was replaced with $h$ and the procedure was repeated starting from the first step; and (6) if $h$ did fulfill the previously defined properties to be an IMF, the procedure was repeated starting again from first step over the residual (*i.e.*, the difference between the original $x$ and all identified IMFs). The process ended when the amplitude of the residual satisfied a predefined stopping criterion (*i.e.*, the residual was below a predetermined level, or it had a monotonic trend) [14]. In this work, we identified only the first IMF as being the one with the fastest characteristic frequency (CF), and we filtered $x$ by subtracting the first IMF from $x$, thus providing an EMD-filtered version of the original series, $x_f$. The CF of the first IMF was computed as the median of the instantaneous frequency of the first IMF obtained from the Hilbert spectrum [19].

### *2.2. SampEn*

Given $x$, we define the pattern of length $L$, $x_L(i)$ as the ordered sequence of $L$ delayed samples, $x_L(i) = [x(i), x(i - 1), \ldots, x(i - L + 1)]$. The pattern $x_L(i)$ is actually a point in the $L$-dimensional embedding space reconstructed with the technique of the lagged coordinates with a delay equal to 1. The pattern $x_L(i)$ can be seen as the sequence formed by the current sample, $x(i)$, and by the sequence of $L$-1 past samples, $x_{L-1}(i - 1) = [x(i - 1), \ldots, x(i - L + 1)]$, *i.e.*, $x_L(i) = [x(i), x_{L-1}(i - 1)]$. Defined as $x_L = \{x_L(i), i = L, \ldots, N\}$ and $x_{L-1} = \{x_{L-1}(i - 1), i = L, \ldots, N\}$ the sets of patterns of length $L$ and $L - 1$ respectively, SampEn estimates the conditional probability that two patterns that are closer than a tolerance $r$ in $x_{L-1}$ remain nearby in $x_L$ [15]. It was calculated as the difference between the negative logarithm of the average probability of finding two patterns closer than $r$ in $L$-dimensional and $(L - 1)$-dimensional embedding space [15]. SampEn was computed with $r$ equal to 0.15-times the standard deviation of the series and with an embedding dimension $L = 3$. SampEn was assessed over $x$, labeled as $\text{SampEn}_x$, and over $x_f$, labeled as $\text{SampEn}_{xf}$, with $x$ = HP or QT.

## 3. Study Population, Experimental Protocol and Data Analysis

### *3.1. Study Population*

All NMCs and MCs belonged to a South African founder population with LQT1 due to the *KCNQ1*-A341V mutation [22,23]. Twelve-lead 24-hour Holter recordings were acquired from 14 NMCs (aged from 19 to 56, median = 36.5; 6 males) and 34 MCs divided in 11 AMCs (aged from 24 to 62, median = 46; 4 males) and 23 SMCs (aged from 16 to 57, median = 39; 9 males). The groups are age-matched according to a Kruskal-Wallis one-way analysis of variance on ranks with $p < 0.05$. Seven AMCs and 22 SMCs were recorded both off BB (BBoff) and on BB (BBon). The remaining 4 AMCs and 1 SMCs were recorded only BBoff. All MCs were recorded BBoff. The number of subjects and the relevant pharmacological condition are summarized in Table 1. The administered drugs were quite homogeneous among patients being in 86% of the cases under propranolol therapy.

The protocol adhered to the principles of the Declaration of Helsinki for medical studies involving human subjects. The protocol was approved by the local ethical committees of the Universities of Vanderbilt, Stellenbosch and Pavia. All enrolled subjects and family members signed an informed consent for clinical and genetic evaluations. Written informed consent was obtained from the next of kin, caretakers or guardians on behalf of minors enrolled in the study.

**Table 1.** Number of subjects undergoing a complete 24-hour Holter recording in each group and relevant pharmacological condition.

| Groups | Number of subjects | Number of subjects acquired only BBoff | Number of subjects acquired both BBoff and BBon |
|---|---|---|---|
| NMC | 14 | 14 | 0 |
| AMC | 11 | 4 | 7 |
| SMC | 23 | 1 | 22 |

NMC = non mutation carrier; BB = beta-blocker therapy; BBoff = off BB; BBon = on BB; AMC = asymptomatic MC; SMC = symptomatic MC.

### *3.2. Data Acquisition*

Seventy-seven 12-lead 24-hour Holter recordings (Mortara Instrument Inc., Milwaukee, WI, USA and Ela Medical, Sorin Group, Arvada, CO, USA) were analyzed. The majority of the recordings were acquired using equipment from Mortara Instrument (*i.e.*, 90%). The sampling rate was 180 Hz with an amplitude resolution of 6.25 μV for the Mortara device, while it was 200 Hz with an amplitude resolution of 10 μV for the Ela Medical device. The lead with the best signal-to-noise ratio was chosen for analysis. The availability of 24-hour Holter recordings permitted the selection of epochs of 5000 consecutive beats during DAY (from 2:00 to 6:00 PM) and NIGHT (from 12:00 PM to 4:00 AM).

### *3.3. Data Analysis*

We computed HP as the temporal distance between two consecutive R-wave peaks of the electrocardiogram. Jitters in the R-wave location were minimized via parabolic interpolation. Then, we took the time distance between the R-wave peak and the T-wave end as an approximation of the QT interval [24]. The end of the T-wave was located when the absolute value of the first derivative over the descending part of the T-wave went below a user-defined threshold computed as 30% of the maximum absolute value of the first derivative computed on the T-wave downslope [24]. The HP and QT intervals were automatically extracted from Holter recordings. Results were manually checked to avoid missing beats or erroneous identifications. HP and QT series were corrected through cubic spline interpolation only in the case of missing beats, the detection of spikes of noise or evident arrhythmias. The number of the corrections was always kept below 5% of the length of the series. HP and QT series were extracted during DAY and NIGHT. The mean of HP, QT and corrected QT (QTc) according to the Bazett's formula [25] were evaluated and labeled as $\mu_{HP}$, $\mu_{QT}$ and $\mu_{QTc}$ respectively. SampEn was computed over the original HP and QT series (*i.e.*, $SampEn_{HP}$ and $SampEn_{QT}$) and from the EMD-filtered HP and QT series (*i.e.*, $SampEn_{HPf}$ and $SampEn_{QTf}$). The CF of the first IMF derived from HP and QT variability was assessed, as well.

### *3.4. Statistical Analysis*

The Wilcoxon signed rank test was utilized to assess the significance of the differences between CF computed over the first IMF of HP and QT series regardless of group, period of analysis and therapy. Two-way repeated measures analysis of variance (one factor repetition, Holm-Sidak test for multiple comparisons) was utilized to assess the significance of the differences between SampEn assessed over the original and EMD-filtered HP and QT series, regardless of group, period of analysis and therapy. One-way analysis of variance (Holm-Sidak test for multiple comparisons), or Kruskal-Wallis one-way analysis of variance on ranks (Dunn's method for multiple comparisons) when appropriate, was applied to check the significance of the differences among BBoff NMCs, AMCs and SMCs during DAY. Two-way repeated measures analysis of variance (one factor repetition, Holm-Sidak test for multiple comparisons) was utilized to assess the significance of the differences between BBoff AMCs and SMCs in relation to the period of analysis (*i.e.*, DAY and NIGHT) and between AMCs and SMCs during DAY in relation to therapy (*i.e.*, BBoff and BBon). Statistical analysis was carried out using a commercial statistical program (Sigmaplot, Systat Software, Inc, Chicago, IL, ver.11.0). $p < 0.05$ was always considered as significant.

## 4. Results

The mean of HP, QT and QTc (*i.e.*, $\mu_{HP}$, $\mu_{QT}$, $\mu_{QTc}$) were reported in Tables 2, 3 and 4 as mean ± standard deviation. $\mu_{HP}$ increased during NIGHT (Table 3) and as a consequence of BB (Table 4) in both AMCs and SMCs. In addition, $\mu_{HP}$ was longer in AMCs than in NMCs (Table 2), and $\mu_{HP}$ lengthened more in response to BB in AMCs than in SMCs (Table 4). $\mu_{QT}$ was longer in MCs (Table 2) and it increased during NIGHT in both AMCs and SMCs (Table 3) and due to BB only in SMCs (Table 4). $\mu_{QTc}$ was longer in MCs (Table 2), and it decreased during NIGHT only in AMCs (Table 3) and due to BB in both AMCs and SMCs (Table 4).

**Table 2.** Mean of HP, QT and QTc in BBoff NMCs and MCs during DAY.

| | **NMC** | **AMC** | **SMC** |
|---|---|---|---|
| $\mu_{HP}$ (ms) | 697.6 ± 100.6 | 847.9 ± 143.8 § | 761.3 ± 95.0 |
| $\mu_{QT}$ (ms) | 317.6 ± 39.2 | 422.2 ± 51.7 § | 408.6 ± 42.4 § |
| $\mu_{QTc}$ ($ms \cdot s^{-1/2}$) | 397.1 ± 71.9 | 461.9 ± 33.9 § | 468.7 ± 33.4 § |

§: $p < 0.05$ *versus* NMCs.

**Table 3.** Mean of HP, QT and QTc in BBoff AMCs and SMCs during DAY and NIGHT.

| | **DAY** | | **NIGHT** | |
|---|---|---|---|---|
| | AMC | SMC | AMC | SMC |
| $\mu_{HP}$ (ms) | 847.9 ± 143.8 | 761.3 ± 95.0 | 1,022.6 ± 136.3 * | 952.4 ± 117.1 * |
| $\mu_{QT}$ (ms) | 422.2 ± 51.7 | 408.6 ± 42.4 | 447.5 ± 42.1 * | 445.3 ± 31.2 * |
| $\mu_{QTc}$ ($ms \cdot s^{-1/2}$) | 461.9 ± 33.9 | 468.9 ± 33.4 | 445.0 ± 30.5 * | 458.6 ± 25.4 |

*: $p < 0.05$ within the same group (*i.e.*, AMCs or SMCs) *versus* DAY.

**Table 4.** Mean of HP, QT and QTc in AMCs and SMCs both BBon and BBoff during DAY.

| | **BBoff** | | **BBon** | |
|---|---|---|---|---|
| | AMC | SMC | AMC | SMC |
| $\mu_{HP}$ (ms) | 855.8 ± 143.5 | 757.9 ± 95.8 | 1,038.2 ± 176.0 $^{@}$ | 927.8 ± 117.2 $^{\#,@}$ |
| $\mu_{QT}$ (ms) | 424.0 ± 57.6 | 406.5 ± 42.1 | 426.7 ± 58.0 | 429.8 ± 29.3 $^{@}$ |
| $\mu_{QTc}$ ($ms \cdot s^{-1/2}$) | 459.4 ± 43.0 | 467.5 ± 33.7 | 418.8 ± 37.2 $^{@}$ | 447.4 ± 28.1 $^{@}$ |

$^{@}$: $p < 0.05$ within the same group (*i.e.*, AMCs or SMCs) *versus* BBoff. #: $p < 0.05$ within the same therapy (*i.e.*, BBoff or BBon) *versus* AMCs subjects.

Figure 1 shows the CF of the first IMF derived from the series of HP (Figure 1a,c,e) and QT (Figure 1b,d,f). The CF of the first IMF computed over the HP series was similar in NMCs, AMCs and SMCs (Figure 1a). It significantly decreased during NIGHT in both AMCs and SMCs (Figure 1c), and it increased as an effect of BB only in AMCs (Figure 1e). The CF of the first IMF computed over the QT series was not influenced by mutation (Figure 1b); it was not modified during NIGHT (Figure 1d), and it was not affected by BB (Figure 1f). It is worth noting that after pooling together the CFs calculated in all individuals (*i.e.*, NMCs and MCs) regardless of the experimental period (*i.e.*, DAY or NIGHT) and therapy (*i.e.*, BBoff or BBon), the CF assessed over the HP series was significantly smaller than that derived from QT series.

**Figure 1.** Bar and grouped bar graphs show the CF of the first IMF computed over HP and QT variability in (**a**,**c**,**e**) and (**b**,**d**,**f**), respectively. The series were derived from BBoff NMCs (gray bars), AMCs (black bars) and SMCs (white bars) during DAY in (**a**) and (**b**), from BBoff AMCs and SMCs during DAY and NIGHT in (**c**) and (**d**) and from AMCs and SMCs both BBoff and BBon during DAY in (**e**) and (**f**). Values are given as the mean plus standard deviation. The symbol * indicates $p < 0.05$.

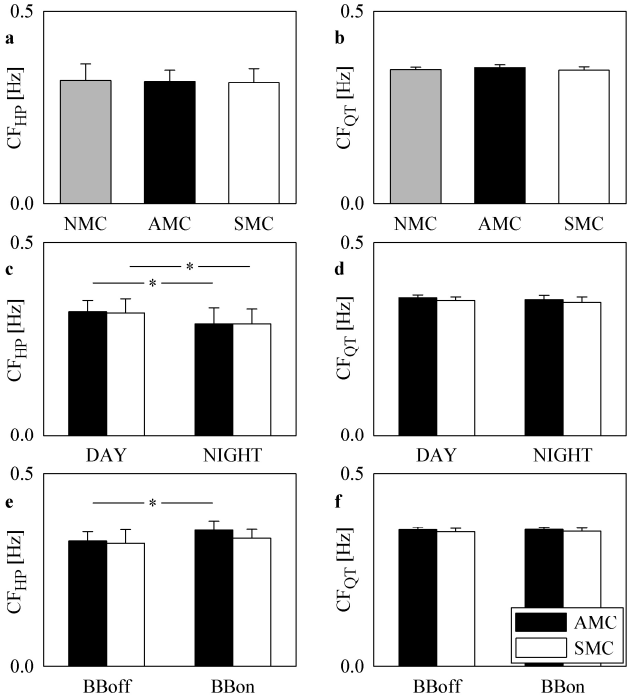

Figure 2 shows SampEn computed over HP and QT variability after pooling together all individuals regardless of the experimental period and therapy. SampEn was computed over the original series $x$ ($SampEn_x$, with $x$ = HP or QT, slash-pattern bars) and over the EMD-filtered version ($SampEn_{xf}$, with $x$ = HP or QT, backslash-pattern bars). SampEn over QT variability was significantly higher than SampEn over HP variability regardless of the processing (*i.e.*, original or filtered series). $SampEn_x$, was significantly higher than $SampEn_{xf}$ regardless of the series (*i.e.*, HP or QT).

**Figure 2.** Grouped bar graphs show results of short-term complexity analysis over HP and QT variability after pooling together all individuals (*i.e.*, NMCs and MCs) regardless of the experimental period (*i.e.*, DAY or NIGHT) and therapy (*i.e.*, BBoff or BBon). SampEn was computed over the original series $x$ ($SampEn_x$, with $x$ = HP or QT, slash-pattern bars) and over the EMD-filtered version ($SampEn_{xf}$, with $x$ = HP or QT, backslash-pattern bars). Values are given as the mean plus standard deviation. The symbol * indicates $p < 0.05$.

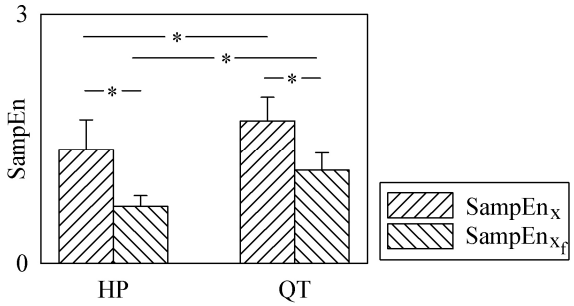


Figure 3 shows SampEn computed over the beat-to-beat variability of HP (Figure 3a,b) and QT (Figure 3c,d) in BBoff NMCs (gray bars) and MCs during DAY. MCs were divided into AMCs (black bars) and SMCs (white bars). SampEn was computed over the original HP and QT series in Figure 3a,c, respectively, and over the EMD-filtered HP and QT versions in Figure 3b,d, respectively. SampEn over the original HP and QT series (Figure 3a,c) and over the EMD-filtered HP versions (Figure 3b) was similar in all considered groups. Conversely, SampEn computed over the EMD-filtered QT series distinguished AMCs from NMCs, while no difference was detected between NMCs and SMCs and between AMCs and SMCs (Figure 3d).

Figure 4 shows SampEn computed over the beat-to-beat variability of HP (Figure 4a,b) and QT (Figure 4c,d) in BBoff MCs during DAY and NIGHT. MCs were divided into AMCs (black bars) and SMCs (white bars). SampEn was computed over the original HP and QT series in Figure 4a,c, respectively, and over the EMD-filtered HP and QT versions in Figure 4b,d, respectively. SampEn computed over the HP variability increased during NIGHT in both AMCs and SMCs (Figure 4a), while this circadian rhythm was not evident in SampEn computed over the EMD-filtered HP variability (Figure 4b). Conversely, while SampEn computed over the HP variability was not able to distinguish AMCs from SMCs during both DAY and NIGHT (Figure 4a), SampEn computed over the EMD-filtered HP variability differentiated AMCs and SMCs during DAY, being larger in SMCs than in AMCs (Figure 4b). SampEn computed over the QT variability decreased during NIGHT in both AMCs and SMCs (Figure 4c), while this circadian rhythm was observed in SampEn calculated over the EMD-filtered QT series only in SMCs (Figure 4d).

**Figure 3.** Bar graphs show the results of short-term complexity analysis over HP and QT variability in (**a**,**b**) and (**c**,**d**), respectively. The series were derived from BBoff NMCs (gray bars) and MCs during DAY. MCs were divided in AMCs (black bars) and SMCs (white bars). SampEn was assessed over the original series in (**a**) and (**c**) and over the EMD-filtered series in (**b**) and (**d**). Values are given as the mean plus standard deviation. The symbol * indicates $p < 0.05$.

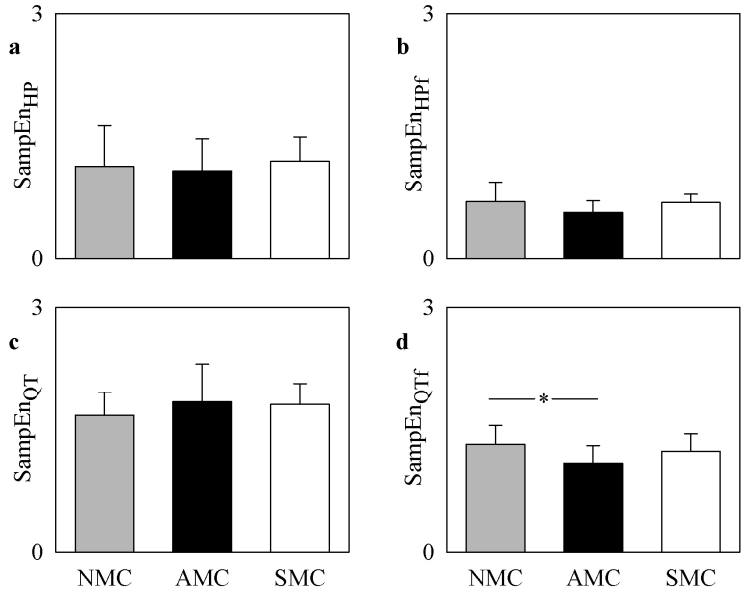


**Figure 4.** Grouped bar graphs show the results of short-term complexity analysis over HP and QT variability in (**a**,**b**) and (**c**,**d**), respectively. The series were derived from BBoff MCs during DAY and NIGHT. MCs were divided in AMCs (black bars) and SMCs (white bars). SampEn was assessed over the original series in (**a**) and (**c**) and over the EMD-filtered series in (**b**) and (**d**). Values are given as the mean plus standard deviation. The symbol * indicates $p < 0.05$.

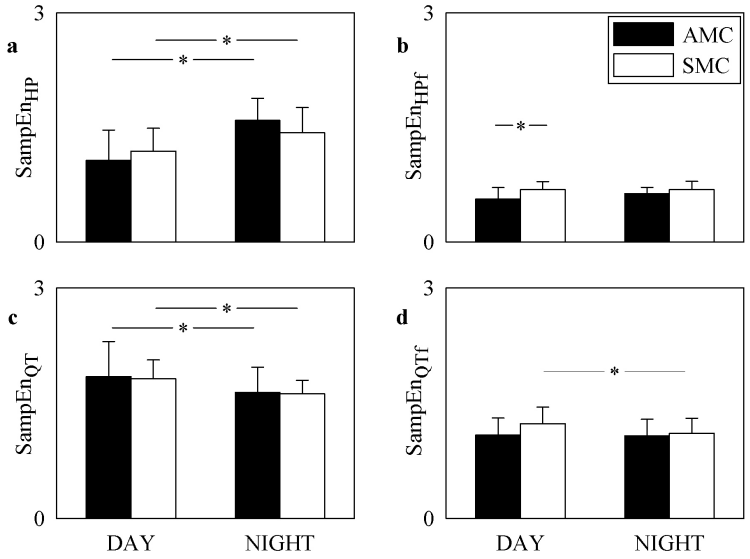

Figure 5 shows SampEn computed over the beat-to-beat variability of HP (Figure 5a,b) and QT (Figure 5c,d) in BBoff and BBon MCs. MCs were divided into AMCs (black bars) and SMCs (white bars). SampEn computed over the HP variability increased BBon in both AMCs and SMCs (Figure 5a), while the effect of BB was not evident in SampEn computed over the EMD-filtered HP variability (Figure 5b). Conversely, while SampEn computed over the HP variability was not able to separate AMCs from SMCs both BBoff and BBon (Figure 5a), SampEn computed over the EMD-filtered HP variability differentiated BBoff AMCs from SMCs, being larger in BBoff SMCs than in BBoff AMCs (Figure 5b). SampEn computed over the QT variability was similar in AMCs and SMCs regardless of the administration of BB (Figure 5c). Conversely, the effect of BB was to decrease SampEn computed over the EMD-filtered QT variability in SMCs, while it remained unmodified in AMCs (Figure 5d).

**Figure 5.** Grouped bar graphs show the results of short-term complexity analysis over HP and QT variability in (**a**,**b**) and (**c**,**d**), respectively. The series were derived from BBoff and BBon MCs during DAY. MCs were divided in AMCs (black bars) and SMCs (white bars). SampEn was assessed over the original series in (**a**) and (**c**) and over the EMD-filtered series in (**b**) and (**d**). Values are given as the mean plus standard deviation. The symbol * indicates $p < 0.05$.

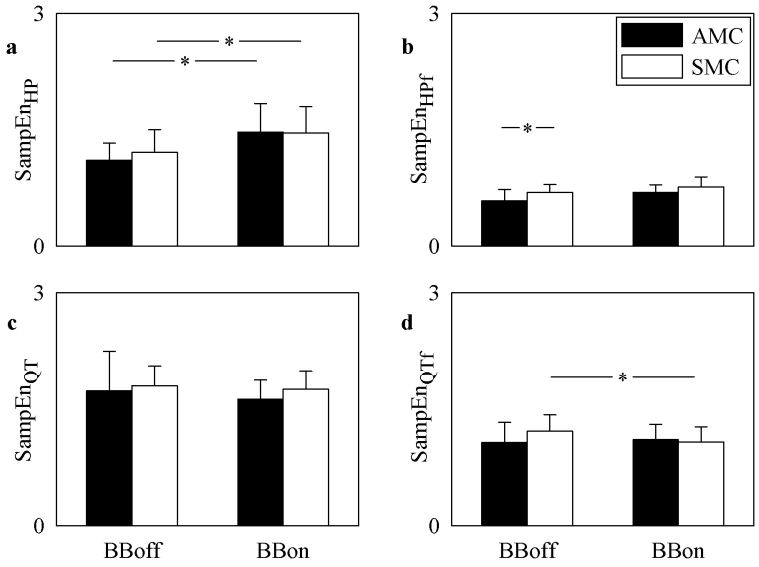


## 5. Discussion

The main findings of this study are: (i) the EMD-based filtering method was helpful to cancel broad-band noise present on QT variability; (ii) when applied to QT variability obtained from 24-hour Holter recordings in LQT1 patients, the EMD-based filtering approach differentiated AMCs from NMCs and detected the effect of BB on SMCs; (iii) when applied to HP variability obtained from 24-hour Holter recordings in LQT1 patients, the EMD-based filtering method cancelled the contribution of vagal modulation to the HP dynamics and enhanced cardiovascular control targeting the sinus node via inputs at frequencies slower than the breathing rate; and (iv) the comparison between complexity indexes derived from the EMD-filtered QT and HP series confirmed the larger

complexity of cardiac control directed to ventricles compared to the one targeting the sinus node as a likely result of inputs modifying QT independently of HP changes.

### *5.1. EMD-Filtered QT Variability Allowed the Separation of AMCs from NMCs*

We have recently found that the complexity of the QT variability at long time scales, as automatically assessed from 24-hour Holter recordings, is smaller in AMCs than in SMCs [10]. This finding is clinically relevant, because it suggests that a low complexity of the sympathetic control directed to ventricles at long time scales, as assessed from QT variability, is a protective factor in LQT1, and markers of QT variability complexity can be utilized to improve risk stratification in LQT1. Of special interest, this result was obtained at long time scales via multiscale entropy [11,12], while traditional complexity analysis at short time scales failed to separate groups [10]. One possible explanation of the different power of the multiscale complexity indexes as a function of the time scale might be the presence of broad-band noise commonly affecting QT variability when automatically derived from 24-hour Holter recordings [13]. The multiscale entropy approach, especially at long time scales, has the intrinsic ability to filter out fast QT variations, thus limiting the effect of broad-band noise on the complexity estimates [10]. The present study tested the hypothesis that even complexity analysis at short time scales, carried out via the traditional estimation of SampEn, has the possibility to distinguish groups with different cardiac risk provided that it is computed over a suitable filtered version of the original QT variability series. Here, the proposed filtering procedure is based on the identification of the fastest IMF, as detected from EMD, and on its subtraction from the original series. This procedure is motivated by the observation that the EMD-filtered version of the QT variability is obtained without *a priori* setting the frequency response of the low-pass filter, because the fastest IMF describes the most rapid temporal scales on a case-by-case basis, thus increasing the flexibility of the low-pass filtering procedure. In agreement with the hypothesis, we found out that SampEn computed over the EMD-filtered QT variability differentiated AMCs from NMCs, while NMCs were similar to the SMCs. The smaller value of SampEn computed over the EMD-filtered QT variability in AMCs is in agreement with the findings obtained from the original QT variability at long time scales in [10] and confirms the observation that a low complexity of the sympathetic control directed to ventricles is protective in LQT1. This result is relevant, because it simplifies the extraction of entropy-based complexity indexes from QT variability (*i.e.*, the multiscale entropy approach is no longer necessary) and favors the inclusion of these markers into risk stratification procedures.

### *5.2. EMD-Filtered QT Variability Allowed the Detection of the Effect of BB*

The ability of the EMD-filtering approach to enhance features pertinent to the sympathetic control directed to ventricles was stressed by the assessment of the effect of BB in MCs. Indeed, before applying the EMD-based filtering procedure, the complexity indexes of QT variability were not able to detect the effect of BB. Conversely, after the application of the EMD-based filtered procedure, the effect of BB over SMCs appeared clearly. Indeed, BB reduced the complexity of the EMD-filtered QT variability, and this reduction, in addition to the prolongation of HP and the reduction of HP variability [3], is protective, because it makes the complexity of the sympathetic control of SMCs more similar to that of the AMCs [10].

### *5.3. EMD-Based Filtering Approach Cancelled Respiratory Sinus Arrhythmia from HP Variability*

The entropy-based complexity of the HP variability at short time scales is under vagal control [20,21,26,27]. This observation was confirmed by the results of the present study. Indeed, SampEn assessed over the original HP variability was significantly increased during NIGHT and in response to BB in both AMCs and SMCs [10]. The effect of the EMD-based filtering procedure was to filter out the respiratory sinus arrhythmia largely responsible for the complexity of the HP variability [20,21]. Indeed, SampEn assessed over the EMD-filtered HP series did not exhibit the circadian rhythmicity and did not vary in response to BB. This finding stresses again the ability of the proposed EMD-based filtering procedure to cancel fast variations present on cardiovascular variability series. The ability of the EMD-based filtering procedure to cancel the respiratory sinus arrhythmia was supported by the CF analysis. Indeed, the CF of the first IMF derived from HP variability was lower during NIGHT due to the slowness of the breathing rate during sleep, and the standard deviation of the CF was quite large due to the high inter-subject variability of the breathing frequency.

### *5.4. EMD-Based Filtering of HP Variability Enhanced Cardiac Control Targeting the Sinus Node at Frequencies Slower Than the Respiratory One*

The most surprising result obtained from this study over the HP variability is that the EMD-based filtering procedure was able to enhance features of the cardiovascular control directed to the sinus node that otherwise would have remained unveiled. Indeed, after the subtraction of the fastest IMF from the original HP variability, we were able to distinguish AMCs from SMCs. Indeed, the complexity of the EMD-filtered HP variability was smaller in AMCs than in SMCs during DAY in absence of BB. This result confirms and extends over the HP variability the observation that a smaller complexity of the sympathetic control is a protective factor in LQT1.

### *5.5. Comparison between Complexity of EMD-Filtered HP and QT Variability*

We confirm here that QT variability is more complex than HP variability [10,28]. This finding was not surprising, because QT variability is more affected by broad-band noise resulting from jitters in delineation of the T-wave offset [24] than HP series. The analysis of the CF of the first IMF derived from QT variability confirmed the intrinsic noisy nature of the QT series compared to the HP one. Indeed, the CF computed over the QT series was higher than that derived from HP series; it was characterized by a lower standard deviation, and it did not vary during NIGHT. It is less trivial to find out that, after canceling the fastest IMF estimated via EMD, the complexity of EMD-filtered QT series remained significantly larger than that of the EMD-filtered HP one. Therefore, we confirm with this analysis the larger complexity of the cardiac control targeting QT compared to that of the cardiac regulation directed to the sinus node. This larger complexity might be the result of inputs capable of modifying QT independently of HP variations and, thus, operating in an asynchronous way with respect to those changing QT through modifications of HP [29–31].

## 6. Conclusions

We proposed an EMD-based filtering procedure to improve the signal-to-noise ratio of QT variability series derived automatically from 24-hour Holter recordings. This procedure is particularly helpful before assessing entropy-based QT variability complexity at short time scales due to the large amount of noise usually affecting this measurement. In the proposed application to a LQT1 population with the founder effect, the procedure allowed the differentiation of AMCs from NMCs and the detection of the effect of BB in SMCs. It is remarkable that this differentiation was not achieved using a largely utilized clinical index, such as QTc. Since similar results were obtained at longer time scales using multiscale entropy analysis in [10], the practical advantage of the proposed methodology was the reduction of the analysis time and approach involvedness, thus favoring the application of complexity indexes into clinically-oriented protocols. Given the generality of the proposed EMD-based filtering procedure, it can be applied to any variability series characterized by a low signal-to-noise ratio due to jitters in the detection of the fiducial points. Therefore, we suggest to exploit this technique even before computing complexity indexes at short time scales from the HP series when the small size of the autonomic modulation leads to negligible HP changes (e.g., in the heart failure population, heart transplanted patients or after administration of a high dose of atropine in healthy individuals). However, this procedure can be profitably exploited even when the HP series is characterized by a high signal-to-noise ratio. In this situation, it cancels the respiratory sinus arrhythmia, thus enhancing features of the cardiovascular control that otherwise might remain unveiled by the dominant vagal modulation. Future studies should check different filtering approaches and entropy-based metrics to better understand the efficacy of the proposed technique compared to techniques exploiting diverse tools. In addition, since a possible limitation of the present study is the low sampling rate of the electrocardiogram, we advocate studies assessing its influence over QT variability and derived complexity parameters.

## Acknowledgments

This study was supported by the Telethon Grant GGP09247 to Peter J. Schwartz, Lia Crotti and Alberto Porta, and by the National Institutes of Health Grant HL068880 to Alfred L. George Jr, Peter J. Schwartz and Lia Crotti.

## Author Contributions

Vlasta Bari: analysis of the data, interpretation of the data, drafting the article, final approval of the version to be published. Andrea Marchi, Beatrice De Maria: analysis of the data, final approval of the version to be published. Giulia Girardengo, Alfred L. George Jr, Paul A. Brink, Lia Crotti, Peter J. Schwartz: acquisition of the data, critical revision of the manuscript, final approval of the version to be published. Sergio Cerutti: critical revision of the manuscript, final approval of the version to be published. Alberto Porta: conception and design of the work, interpretation of the data, drafting the article, critical revision of the manuscript, final approval of the version to be published. All authors have read and approved the final manuscript.

## List of Abbreviations

| | |
|---|---|
| LQT1 | long QT syndrome type 1 |
| HP | heart period |
| QT | interval from Q-wave onset to T-wave end |
| QTc | corrected QT |
| MC | mutation carrier |
| NMC | non-mutation carrier |
| AMC | asymptomatic MC |
| SMC | symptomatic MC |
| DAY | daytime |
| NIGHT | nighttime |
| BB | beta-blocker therapy |
| BBoff | off BB |
| BBon | on BB |
| EMD | empirical mode decomposition |
| IMF | intrinsic mode function |
| CF | characteristic frequency |
| SampEn | sample entropy |
| $\mu_{HP}$ | HP mean |
| $\mu_{QT}$ | QT mean |
| $\mu_{QTc}$ | QTc mean |

## Conflicts of Interest

The authors declare no conflict of interest.

## References

1. Schwartz, P.J.; Crotti, L. QTc Behavior During Exercise and Genetic Testing for the Long-QT Syndrome. *Circulation* **2011**, *20*, 2181–2184.
2. Schwartz, P.J.; Priori, S.G.; Spazzolini, C.; Moss, A.J.; Vincent, G.M.; Napolitano, C.; Denjoy, I.; Guicheney, P.; Breithardt, G.; Keating, M.T.; *et al.* Genotype-phenotype correlation in the long-QT syndrome-Gene specific triggers for life threatening arrhythmias. *Circulation* **2001**, *103*, 89–95.
3. Schwartz P.J.; Ackerman M.J. The long QT syndrome. A transatlantic clinical approach to diagnosis and therapy. *Eur. Heart J.* **2013**, *34*, 3109–3116.
4. Crotti, L.; Lundquist, A.L.; Insolia, R.; Pedrazzini, M.; Ferrandi, C.; De Ferrari, G.M.; Vicentini, A.; Yang, P.; Roden, D.M.; George, A.L.; Schwartz, P.J. KCNH2-K897T is a genetic modifier of latent congenital long QT syndrome. *Circulation* **2005**, *112*, 1251–1258.
5. Crotti, L.; Monti, M.C.; Insolia, R.; Peljto, A.; Goosen, A.; Brink, P.A.; Greenberg, D.A.; Schwartz, P.J.; George, A.L. NOS1AP is a genetic modifier of the long-QT syndrome. *Circulation* **2009**, *120*, 1657–1663.

6. Amin, A.S.; Giudicessi, J.R.; Tijsen, A.J.; Spanjaart, A.M.; Reckman, Y.J.; Klemens, C.A.; Tanck, M.W.; Kapplinger, J.D.; Hofman, N.; Sinner, M.F.; *et al.* Variants in the 3' untranslated region of the KCNQ1-encoded Kv7.1 potassium channel modify disease severity in patients with type 1 long QT syndrome in an allele-specific manner. *Eur. Heart J.* **2012**, *33*, 714–723.
7. Duchatelet, S.; Crotti, L.; Peat, R.; Denjoy, I.; Itoh, H.; Berthet, M.; Ohno, S.; Fressart, V.; Monti, M.C.; Crocamo, C.; *et al.* Identification of a KCNQ1 polymorphism acting as a protective modifier against arrhythmic risk in the long QT syndrome. *Circ. Cardiovasc. Genet.* **2013**, *6*, 354–361.
8. Schwartz, P.J.; Vanoli, E.; Crotti, L.; Spazzolini, C.; Ferrandi, C.; Goosen, A.; Hedley, P.; Heradien, M.; Bacchini, S.; Turco, A.; *et al.* Neural control of heart rate is an arrhythmia risk modifier in long QT syndrome. *J. Am. Coll. Cardiol.* **2008**, *51*, 920–929.
9. Crotti, L.; Spazzolini, C.; Porretta, A.P.; Dagradi, F.; Taravelli, E.; Petracci, B.; Vicentini, A.; Pedrazzini, F.; La Rovere, M.T.; Vanoli, E.; *et al*. Vagal reflexes following an exercise stress test. A simple clinical tool for gene-specific risk stratification in the long QT syndrome. *J. Am. Coll. Cardiol.* **2012**, *60*, 2515–2524.
10. Bari, V.; Valencia, J.F.; Vallverdú, M.; Girardengo, G.; Marchi, A.; Bassani, T.; Caminal, P.; Cerutti, S.; George, A.L.; Brink, P.A.; *et al.* Multiscale complexity analysis of the cardiac control identifies asymptomatic and symptomatic patients in long QT syndrome type 1. *PLoS ONE*, **2014**, *9*, doi:10.1371/journal.pone.0093808.
11. Costa, M.; Goldberger, A.L.; Peng, C.-K. Multiscale entropy analysis of complex physiologic time series. *Phys. Rev. Lett.* **2002**, *89*, doi:10.1103/PhysRevLett.89.068102.
12. Valencia, J.F.; Porta, A.; Vallverdù, M.; Clarià, F.; Baranowski, R.; Orlowska-Baranowska, E.; Caminal, P. Refined multiscale entropy: Application to 24-h Holter recordings of heart period variability in healthy and aortic stenosis subjects. *IEEE Trans. Biomed. Eng.* **2009**, *56*, 2202–2213.
13. Baumert, M.; Starc, V.; Porta, A. Conventional QT variability measurement *vs*. template matching techniques: comparison of performance using simulated and real ECG. *PLoS ONE* **2012**, *7*, doi:10.1371/journal.pone.0041920.
14. Huang, N.E.; Zheng, S.; Long, S.R.; Wu, M.C.; Shih, H.H.; Zheng, Q.; Yen, N.-C.; Tung, C.C.; Liu, H.H. The empirical mode decomposition and the Hilbert spectrum for nonlinear and non-stationary time series analysis. *Proc. R. Soc. A* **1998**, *454*, 903–995.
15. Richman, J.S.; Moorman, J.R. Physiological time-series analysis using approximate entropy and sample entropy. *Am. J. Physiol.* **2000**, *278*, 2039–2049.
16. Balocchi, R.; Menicucci, D.; Santarcangelo, E.; Sebastian, L.; Gemignani, A.; Ghelarducci, B.; Varanini, M. Deriving the respiratory sinus arrhythmia from the heartbeat time series using empirical mode decomposition. *Chaos Solit. Fract.* **2004**, *20*, 171–177.
17. Neto, E.S.; Custaud, M.A.; Cejka, J.C.; Abry, P.; Frutoso, J.; Gharib, C.; Flandrin, P. Assessment of cardiovascular autonomic control by the empirical mode decomposition. *Methods Inf. Med.* **2004**, *43*, 60–65.
18. Echeverría, J.C.; Crowe, J.A.; Woolfson, M.S.; Hayes-Gill, B.R. Application of empirical mode decomposition to heart rate variability analysis. *Med. Biol. Eng. Comput.* **2001**, *39*, 471–479.

19. Maestri, R.; Pinna, G.D.; Accardo, A.; Allegrini, P.; Balocchi, R.; D'Addio, G.; Ferrario, M.; Menicucci, D.; Porta, A.; Sassi, R.; *et al.* Nonlinear indices of heart rate variability in chronic heart failure patients: redundancy and comparative clinical value. *J. Cardiovasc. Electrophysiol.* **2007**, *18*, 425–433.
20. Porta, A.; Castiglioni, P.; Bari, V.; Bassani, T.; Marchi, A.; Cividjian, A.; Quintin, L.; Di Rienzo, M. K-nearest-neighbor conditional entropy approach for the assessment of short-term complexity of cardiovascular control. *Physiol. Meas.* **2013**, *34*, 17–33.
21. Porta, A.; Gnecchi-Ruscone, T.; Tobaldini, E.; Guzzetti, S.; Furlan, R.; Montano, N. Progressive decrease of heart period variability entropy-based complexity during graded head-up tilt. *J. Appl. Physiol.* **2007**, *103*, 1143–1149.
22. Brink, P.A.; Crotti, L.; Corfield, V.; Goosen, A.; Durrheim, G.; Hedley, P.; Heradien, M.; Geldenhuys, G.; Vanoli, E.; Bacchini, S.; *et al.* Phenotypic variability and unusual clinical severity of congenital long-QT syndrome in a founder population. *Circulation* **2005**, *112*, 2602–2610.
23. Brink, P.A.; Schwartz, P.J. Of founder populations, long QT syndrome, and destiny. *Heart Rhythm* **2009**, *6*, 25–33.
24. Porta, A.; Baselli, G.; Lombardi, F.; Cerutti, S.; Antolini, R.; Del Greco, M.; Ravelli, F.; Nollo, G. Performance assessment of standard algorithms for dynamic R-T interval measurement: Comparison between R-Tapex and R-Tend approach. *Med. Biol. Eng. Comput.* **1998**, *36*, 35–42.
25. Bazett, H.C. An analysis of the time-relations of electrocardiograms. *Heart* **1920**, *7*, 353–370.
26. Turianikova, Z.; Javorka, K.; Baumert, M.; Calkovska, A.; Javorka, M. The effect of orthostatic stress on multiscale entropy of heart rate and blood pressure. *Physiol. Meas.* **2011**, *32*, 1425–1437.
27. Porta, A.; Faes, L.; Masé, M.; D'Addio, G.; Pinna, G.D.; Maestri, R.; Montano, N.; Furlan, R.; Guzzetti, S.; Nollo, G.; *et al.* An integrated approach based on uniform quantization for the evaluation of complexity of short-term heart period variability: Application to 24h Holter recordings in healthy and heart failure humans. *Chaos* **2007**, *17*, doi:10.1063/1.2404630.
28. Baumert, M.; Javorka, M.; Seeck, A.; Faber, R.; Sanders, P.; Voss, A. Multiscale entropy and detrended fluctuation analysis of QT interval and heart rate variability during normal pregnancy. *Comput. Biol. Med.* **2012**, *42*, 347–352.
29. Porta, A.; Tobaldini, E.; Gnecchi-Ruscone, T.; Montano, N. RT variability unrelated to heart period and respiration progressively increases during graded head-up tilt. *Am. J. Physiol.* **2010**, *298*, 1406–1414.
30. Negoescu, R.; Dinca-Panaitescu, S.; Filcescu, V.; Ionescu, D.; Wolf, S. Mental stress enhances the sympathetic fraction of QT variability in an RR-independent way. *Integr. Physiol. Behav. Sci.* **1997**, *32*, 220–227.
31. Browne, K.F.; Prystowsky, E.; Heger, J.J.; Zipes, D.P. Modulation of Q-T interval by the autonomic nervous system. *PACE-Pacing Clin. Electrophysiol.* **1983**, *6*, 1050–1055.